

Tracking Back the Solar Wind to its Photospheric Footpoints from *Wind* Observations — A Statistical Study

Chong Huang¹ · Yihua Yan¹ · Gang Li^{1,2} ·
Yuanyong Deng¹ · Baolin Tan¹

© Springer

Abstract

It is of great importance to track the solar wind back to its photospheric source region and identify the related current sheets; this will provide key information for investigating the origin and predictions of the solar wind. We report a statistical study relating the photospheric footpoint motion and *in-situ* observation of current sheets in the solar wind. We used the potential force-free source–surface (PFSS) model and the daily synoptic charts to trace the solar wind back from 1 AU, as observed by the *Wind* spacecraft, to the solar surface. As the footpoints move along the solar surface we obtain a time series of the jump times between different points. These jumps can be within a cell and between adjacent cells. We obtained the distribution of the jump times and the distribution for a subset of the jump times in which only jumps between adjacent cells were counted. For both cases, the distributions clearly show two populations. These distributions are compared with the distribution of *in-situ* current sheets reported in an earlier work of Miao, Peng, and Li (*Ann. Geophys.* **29**, 237, 2011). Its implications on the origin of the current sheets are discussed.

Keywords: Solar wind, Magnetic fields, Current Sheets, Supergranulation

1. Introduction

Magnetohydrodynamic (MHD) turbulence intermittency in the solar wind is an important topic in space plasma research Tu and Marsch (1995); Goldstein, Roberts, and Matthaeus (1995); Bruno and Carbone (2005). The intermittency emerges because the magnetic fields and velocity fluctuations are not scale invariant as conjectured in the hydrodynamic turbulence theory of Kolmogorov

¹ Key Laboratory of Solar Activity, National Astronomical
Observatories of Chinese Academy of Sciences, Beijing,
China, 100012
email: chuang@nao.cas.cn

² Department of Physics and CSPAR, University of Alabama
in Huntsville, AL, 35899, USA

(1941). An important intermittent structure in the solar wind is the current sheet, which is a two-dimensional structure where the magnetic-field directions change significantly. Earlier work on the existence of current sheets and their effects on solar-wind MHD turbulence has been carried out by Veltri and Mangeney (1999). These authors applied the Haar wavelets technique to calculate the power spectra and structure functions of the solar wind using fluid velocity and magnetic-field data from the *International Sun-Earth Explorer* (ISEE) space experiment. The temporal separations in their study range from one minute to about one day. They suggested that the most important intermittent structures in the solar wind are shocks and current-sheet-like structures.

Bruno *et al.* (2001) studied current sheets using *Helios 2* data and suggested for the first time that current sheets were ubiquitous in the solar wind and probably are boundaries of flux tubes. In a subsequent work, Bruno *et al.* (2004) furthermore obtained the probability distribution functions (PDF) of the solar-wind fluctuations and confirmed the results of Bruno *et al.* (2001): there appeared to be two populations of current sheets in the solar wind, one of which was flux-tube boundaries.

Alternative views about the origin of current sheets also exist. For example, numerical MHD simulations by Zhou, Matthaeus, and Dmitruk (2004) and Chang, Tam, and Wu (2004) showed that current sheets can emerge from the dynamical evolution of the nonlinear interactions of the solar-wind MHD turbulence. All of these studies suggested that the current sheet is an intrinsic property of the solar-wind MHD turbulence. In contrast, Borovsky (2008) examined one-year magnetic-field data from the *Advanced Composition Explorer* (ACE) spacecraft and found that the population of the angle between two magnetic field measurements with a separation of 64 seconds showed a clear signature of two populations, supporting the earlier claim of Bruno *et al.* (2001). Borovsky (2008) suggested that these current sheets are “magnetic walls” of flux tubes in the solar wind and are relic structures that can be traced back to the surface of the Sun. In this scenario, current sheets are carried outward by the solar wind as passive structures. The plasma in the solar wind is bundled in “spaghetti-like” flux tubes Bartley *et al.* (1966); McCracken and Ness (1966); Mariani *et al.* (1973).

Recently, Trenchi *et al.* (2013b) analyzed the *in-situ* observations of solar energetic particles (SEPs) and found several SEP modulation signatures in local magnetic field and/or plasma parameters. From studying the magnetic helicity, it is possible to identify magnetic boundaries associated with variations of plasma parameters, which are thought to represent the borders between adjacent magnetic-flux tubes. The authors found that SEP dispersionless modulations are generally associated with such magnetic boundaries. They also analyzed the local magnetic field topology in depth by applying a GradC-Shafranov reconstruction Trenchi *et al.* (2013b), and found that flux ropes or current sheets with a more complex field topology are generally associated with the maxima in the SEP counts. This association shows that the SEPs propagate within these structures and cannot escape from them because of their much smaller gyration radii relative to the transverse dimensions of those structures Trenchi *et al.* (2013a).

To identify current sheets in the solar wind, Li (2007; 2008) developed a systematic method to obtain the exact locations of individual current sheets. Li, Lee, and Parks (2008) applied this method to data of the *Cluster* spacecraft in an attempt to identify the origin of these current sheets. The *Cluster* spacecraft was chosen because its orbit traverses both the solar wind and Earth's magnetosphere. Li, Lee, and Parks (2008) found that unlike in the solar wind, there is no clear signature of current sheets in Earth's magnetosphere. This result is a natural outcome when current sheets of solar wind are indeed relic structures originating from the solar surface. Extending the work of Li (2007; 2008), Miao, Peng, and Li (2011) developed an automatic current-sheet identification procedure and examined the solar-wind magnetic-field data of *Ulysess*. Their results are consistent with those of Borovsky (2008).

To confirm whether current sheets are boundaries of flux tubes that originate from the solar surface, one straightforward approach is to trace the solar wind back from *in-situ* observations near Earth's orbit at 1 AU to the solar surface and examine if, for those current sheets observed *in-situ*, there are corresponding footpoint jumps between adjacent photospheric cells. To identify these photospheric cells, Huang *et al.* (2012) used a watershed algorithm and the magnetogram observed by the *Solar and Heliospheric Observatory* (SOHO)/*Michelson Doppler Imager* (MDI; Scherrer *et al.* (1995)). After identifying the photospheric cells, one can then examine how the footpoints jump within and between these cells. If the two different jump times have different distributions, we may deduce that the current sheets originate from two different mechanisms, and when the two different jump times have the same distribution, the same generation mechanism of the current sheets can be considered.

The solar wind from near Earth's orbit to the solar surface has been back-traced before. For example, to study the quadrupole distortions of the heliospheric current sheet and compare the K-coronameter observations with a potential-field model, Bruno, Burlaga, and Hundhausen (1982; 1984) used the solar-wind tracing-back process during the period from May 1976 to May 1977. Neugebauer *et al.* (1998) used the data obtained by *Ulysess* and *Wind* in early 1995 to trace back solar wind structures to the source surface and then map them back to the photosphere. They found that the footpoints of the open field-lines calculated from the model are generally consistent with observations in the He 10830 Å line of locations of coronal holes. Recently, in an attempt to make a physical connection between the Equatorial Coronal Hole (ECH) and the solar wind observed at about 1 AU, McIntosh *et al.* (2010) used the data from ACE to track the solar wind back to the solar surface using the Potential Field Source Surface (PFSS) model Schatten, Wilcox, and Ness (1969); Altschuler and Newkirk (1969).

In mapping the solar wind back to the Sun, it was assumed that the coronal magnetic field is quasi-stationary Schatten, Wilcox, and Ness (1969); Altschuler and Newkirk (1969). This allows one to apply the PFSS model using one synoptic chart. However, such methods will inevitably produce some artificial bias towards the two sides of the magnetogram, because some source regions and magnetic-field lines do not last for one Carrington Rotation (CR). In a recent work, Sun *et al.* (2012) used the nonlinear force-free field (NLFFF) extrapolation

to demonstrate that the change in the photospheric and coronal field is morphologically consistent with the “magnetic implosion” conjecture; this change is supported by the coronal-loop retraction observed by the *Solar Dynamic Observatory* (SDO)/*Atmospheric Imaging Assembly* (AIA: Lemen *et al.* (2012)).

Instead of using a single synoptic chart, we used in our study the daily synoptic chart as the boundary for the PFSS model. This method improves the accuracy of the two sides of the synoptic chart, and consequently the locations of the photospheric footpoints. We applied this revised model to map the solar wind back to the solar surface using *in-situ* data from *Wind* and ACE observations, and then calculated the jump times between adjacent footpoints, and the jump times of adjacent footpoints that jump across the boundaries of cells.

If the current sheets in solar wind are relic structures that originate from the solar surface, one can expect that the waiting-time statistics of these *in-situ* current sheets and that of the jump time between adjacent cells is similar. Likewise, the distribution between all jump times and that of footpoints that cross the boundaries of cells will be similar. In this work we performed such a statistical comparison. To our knowledge, this is the first attempt of a semi-quantitative study to relate the solar-surface observations with *in-situ* solar wind observations. The article is organized as follows: Section 2 introduces the data analysis procedure and the data reduction, the results are presented in Section 3, and the discussion and main conclusions are presented in Section 4.

2. Observations and Data Reduction

2.1. Data Selection

To accurately track the solar wind back from near Earth’s orbit (at about 1 AU) to the solar source surface (*e.g.* $2.5 R_{\odot}$), in the extrapolation of the coronal magnetic field, we generally take the $2.5 R_{\odot}$ for the solar source surface, where R_{\odot} is the radius of the Sun. Therefore, it is necessary to select quasi-stationary periods of the solar wind to perform our analysis.

We focus on studying the minimum of the solar cycle when the solar wind and solar magnetic field can be regarded as quasi-stationary (Bruno, Burlaga, and Hundhausen, 1982, 1984; Neugebauer *et al.*, 1998); furthermore, transient disturbances, such as CMEs, are relatively inactive Miao, Peng, and Li (2011). We selected the data during the declining phase of Solar Cycle 23 from 2004 to 2005 (CR2012–CR2037) obtained by the ACE and *Wind* spacecrafts. The ACE spacecraft is located at the Lagrangian point (The Sun–Earth L_1), while the *Wind* spacecraft spends some of its time within Earth’s magnetosphere. For ACE, the plasma data were obtained by the *Solar Wind Electron, Proton and Alpha Monitor* (SWEPAM), and the magnetic-field data were obtained by the *Magnetometer* (MAG: McComas *et al.* (1998)). For *Wind*, the plasma and magnetic-field data were obtained by the *Solar Wind Experiment* (SWE) and the *Magnetic Field Investigation* (MFI) Ogilvie *et al.* (1995); Lepping *et al.* (1995), respectively.

The present analysis is based on one-hour averages of the *in-situ* observation data.

2.2. Tracking the Solar Wind from *In-Situ* Back to the Source Surface

We discuss the back-tracking procedure of the solar wind from 1 AU observation to the source surface. We assumed that the source surface is located at about $2.5 R_{\odot}$ from the center of the Sun.

To obtain the accurate positions of footpoints at the source surface, we first transformed the position of the spacecraft ACE and *Wind* from the Geocentric Solar Ecliptic system (GSE) to the Carrington coordinate system Hapgood (1992) and obtained the heliographic latitude and longitude of *Wind* and ACE. The latitude of the footpoint is approximately equal to the heliographic latitude of the spacecraft, and the longitude of the footpoint is then obtained by taking into account the effect of solar-wind propagation.

We calculated the propagation time in the Heliocentric Earth Ecliptic (HEE) coordinate system where the x -axis is along the Sun–Earth line and the z -axis points to the ecliptic north pole. P_x denotes as the distance between the spacecraft and the center of the Sun, V_x the radial velocity of the solar wind observed at the spacecraft. We furthermore assumed V_x to be a constant during the propagation. The propagation time of the solar wind from the spacecraft to the source surface is then

$$\Delta t = \frac{P_x - 2.5R_s}{V_x}, \quad (1)$$

and the offset to the longitude produced from the solar wind propagation is

$$D = \frac{360^\circ}{27.2753 \times 86400} \Delta t. \quad (2)$$

Adding this offset, we obtain the actual positions of footpoints that track back from *in-situ* to the solar source surface.

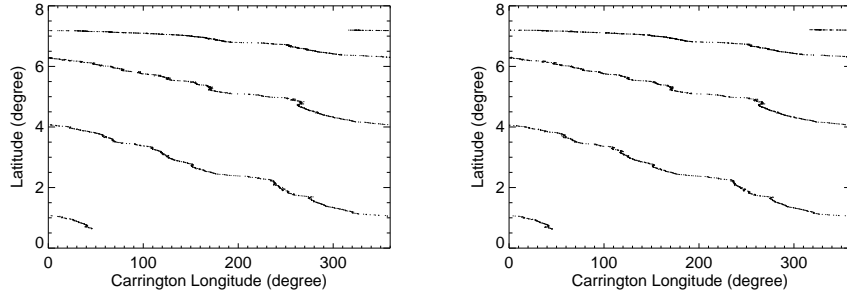


Figure 1. Heliographic latitude and longitude of the source region of the solar wind observed by the *Wind* (left) and the ACE (right) spacecraft during CR 2071–2073. The solar-wind speed is assumed to be constant between the Sun and the spacecraft.

Figure 1 shows a map of the latitudes and Carrington longitudes of the mapped-back locations on the solar source surface of the solar wind observed by *Wind* and ACE with a propagation time calculated from the observed speeds assuming constant-speed radial flow between the source regions and the spacecraft.

The coronal-hole data are only available after September 2006, and considering that the period (2004–2008) is in the declining phase of Solar Cycle 23, we selected the data from CR 2071 to CR 2073 (from 11 June 2008 to 5 September 2008 at *in-situ*) to compare with the coronal-hole plot. We used one-hour solar-wind speed data and obtain 24 footpoints at the source surface every day. From Figure 1, we can see that the footpoints at the source surface jump smoothly, which agrees with the result of Neugebauer *et al.* (1998). Note that the two spacecraft gradually drift to north in the studied period McIntosh *et al.* (2010); Neugebauer *et al.* (1998).

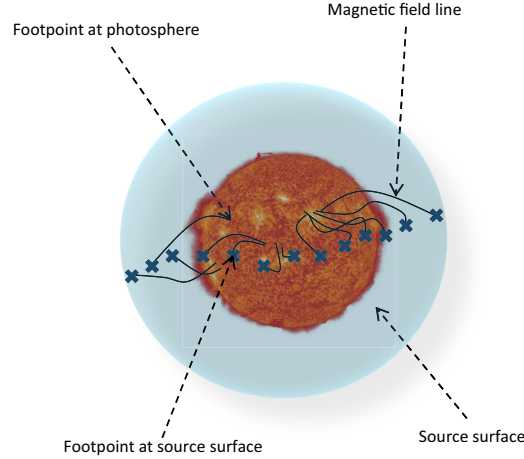


Figure 2. The mapping from the source surface to the photosphere.

2.3. Tracking the Solar Wind Back from the Source Surface to the Photosphere

The second step is to trace back the solar wind from the source surface to the photosphere. We used the PFSS model (Schatten, Wilcox, and Ness (1969) and Altschuler and Newkirk (1969)) in this step. In this model, the coronal magnetic field is assumed to be quasi-stationary and is described by a potential field that can be approximated by an expansion to series of spherical harmonics. We used the standard PFSS package included in SolarSoft (Schrijver, 2001, 2003). Figure 2 is a map of field lines that trace back from the source surface (located at $2.5 R_{\odot}$) to the solar photosphere. The thick crosses on the translucent blue sphere are the footpoints on the source surface. The solid lines are magnetic-field lines extrapolated using the PFSS model.

For the extrapolation, we used the SOHO/MDI synoptic chart. To relate a footpoint to a particular magnetic cell, we superposed the footpoints on the synoptic chart. The Carrington synoptic chart is a collection of the center of full-disk magnetograms during one Carrington rotation. These synoptic charts have been reconstructed using re-calibrated magnetogram data Scherrer *et al.* (1995). Figure 3 shows the synoptic chart from SOHO/MDI during CR 2072.

The diamonds and squares show the footpoints that are traced back from the source surface using the *Wind* and ACE data, respectively. The footpoints do not move smoothly across the synoptic chart. Instead, they undergo sudden jumps on the synoptic chart, part of them overlapping on the boundaries of the coronal holes. A large portion of the footpoints originate from coronal holes. We compared this with the Integral Models Synoptic Coronal Hole Plot, which is shown at the bottom of Figure 3, and found that most of the footpoints are located either at the boundaries or in the coronal holes. This result is consistent with those of McIntosh, Leamon, and de Pontieu (2011) and Neugebauer *et al.* (1998). Note that most of the footpoints deduced from *Wind* are the same as those deduced from ACE. This is expected because the separation between ACE and *Wind* is small.

In the following, we use the data observed by the *Wind* spacecraft to calculate the jump times of the footpoints. The jump time t , in Carrington coordinates, is equivalent to the longitudinal difference between the two adjacent footpoints divided by the solar rotation speed:

$$t = \frac{|s2 - s1|}{V_{rs}}, \quad (3)$$

where $s1$ and $s2$ are the longitude of adjacent footpoints, and V_{rs} is the rotation speed of the Sun.

Note that toward the two sides of the magnetogram, the tracing process needs to be calculated carefully because the source region and field line may only last a fraction of a Carrington rotation. In the two sides of the daily synoptic chart, the magnetic field of the region changes faster than the normal level, which may lead to variations of the extrapolated field lines. Thus, when we track back along these field lines, the backtracked footpoints are not static. To extend this model, we used the daily synoptic chart as the boundary of PFSS model. In this model, the field lines extrapolated from the two sides of the daily synoptic chart could be in their actual condition, therefore we can trace the field lines more accurately. Applying this extended model, we mapped the solar wind back to the solar surface with *Wind* and ACE data, from the source surface to the solar photosphere. We found that most of the footpoints that trace the field lines extrapolated from the daily synoptic chart are clustered. Therefore we selected the relatively stable daily footpoints, whose variance is less than 1σ during one CR, to calculate the jump times of adjacent footpoints.

Figure 4 presents the traced-back footpoints superimposed on the magnetic cells, which were identified with the watershed algorithm. Some of the sky-blue footpoints are inside the same magnetic cell; the others are at the boundary of the cell. The jump times of all adjacent footpoints were calculated, and we tallied the statistical results in two ways: the first way was to examine the jump times between all adjacent footpoints, regardless of whether they were within the same cell or in different cells; the second way was to count only the jump times between different cells.

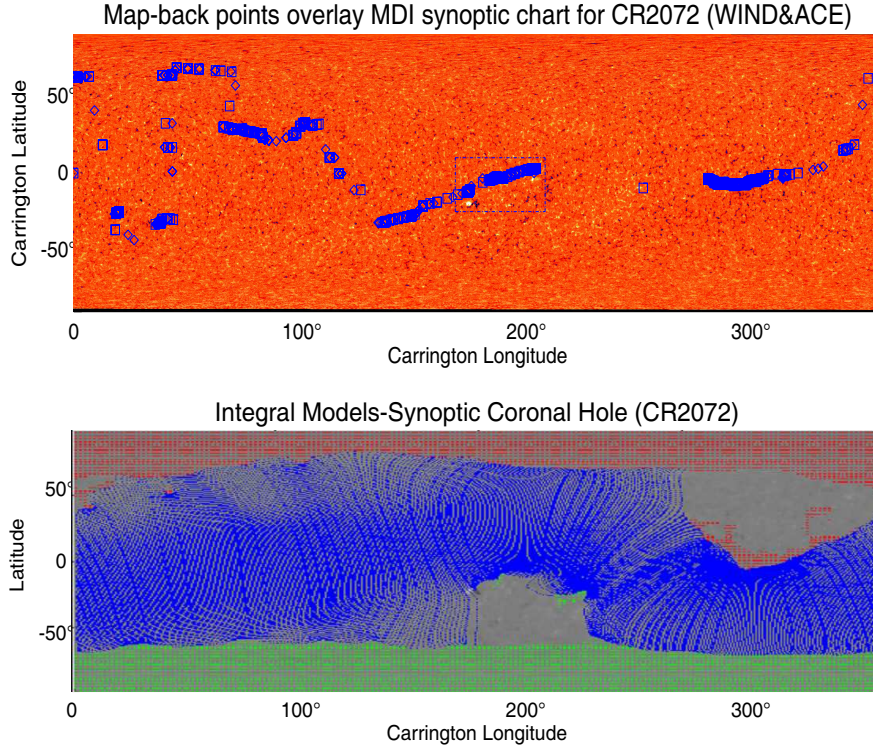


Figure 3. Upper panel: Synoptic chart from SOHO/MDI during CR 2072. The diamonds and squares show the footpoints that trace back from the positions of source surface with *Wind* and ACE data, respectively; the white dashed line represents the solar equator. The detail of the blue frame region is shown in Figure 4. Lower panel: The Integral Models Synoptic Coronal Hole from NSO/GONG, the polarities of both the open ecliptic-plane flux and the coronal holes are indicated by the same color code: green for positive polarity and red for negative polarity. The tallest closed-flux trajectories are plotted in blue.

3. Results

In the scenario where the solar wind contains numerous flux tubes (*e.g.* Bruno *et al.* (2001); Borovsky (2008); Li (2008); Li, Lee, and Parks (2008)), the solar-wind plasma resides in different flux tubes, which originate from the top of the magnetic carpet. These flux tubes wander around their footpoints while they propagate out during their merging or splitting. The time scale of the merging and splitting is currently unclear, however. If the merging and splitting time scales of these flux tubes are much longer than the propagating time of the solar wind from the Sun to Earth, *i.e.* if they can survive intact beyond 100 hours, then they can be regarded as nonevolving fossil structures of magnetic cells near the photosphere. In this case, one expects the observation of these flux tubes at 1 AU to resemble their footpoints on the solar surface. In particular, the crossings of flux tubes at 1 AU are expected to correspond to the jump between magnetic cells on the solar surface. Statistically, we therefore expect that the waiting times

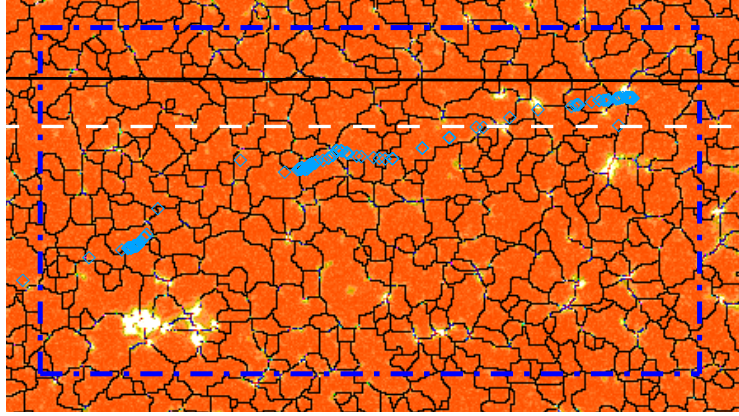


Figure 4. Enlarged images for the window framed in Figure 3. The longitude of the region is from 160° to 210° , and the latitude is from -25° to 10° . The white dashed line is the solar equator, the sky-blue diamonds are footpoints, that are traced back by employing *Wind* data, and the black solid line is the projection point of the *Wind* spacecraft during CR 2072.

of current sheets are similar to the footpoint jump times between magnetic cells at the photosphere.

Miao, Peng, and Li (2011) recently used *Ulysses* data to examine the PDF of the waiting times of current sheets in the solar wind. We examine the PDF of the jump times of the traced-back solar-wind footpoints. We also note that several authors have reported that the lifetime of the supergranules (candidates for the magnetic cells) is about one day Wang and Zirin (1989); Hirzberger *et al.* (2008). This justifies our choice of using one-hour data for our statistical analysis.

For the reasons discussed in Section 2.3, and because the daily synoptic chart can reflect the transient magnetogram more accurately, we used the daily synoptic charts to extrapolate the magnetic-field lines and then traced back the footpoints that are located on the source surface to the photosphere. Compared with one Carrington synoptic chart, it is more accurate for the tracing-back process to apply about 27 daily synoptic charts in one Carrington rotation. Because the daily tracing-back processes are relatively independent, we calculated the jump time of adjacent footpoints in each tracing-back process during one Carrington rotation. Thus, this data-processing produces 26 more jump cases than the actual physical scenario. In this statistical analysis, we scaled the data to meet the actual scenarios by using statistical averaging.

The left panel of Figure 5 shows the statistical distribution of the footpoint jump times of solar wind during the years 2004 (a), 2005 (b), and 2004–2005 (c), respectively. Here, the x -axis is the logarithm of time, and the y -axis is the logarithm of the probability density. The distributions are best-fitted by two log-normal functions (shown as blue and red curves): one at short jump times, the other one at long jump times. The right panels of Figure 5 show the probability distributions of the waiting times of current sheets with all deflection angles observed *in-situ* by Miao, Peng, and Li (2011).

In the left panel of Figure 5, these three distributions are approximately log-normal distributions at short jump times. Log-normal distributions were

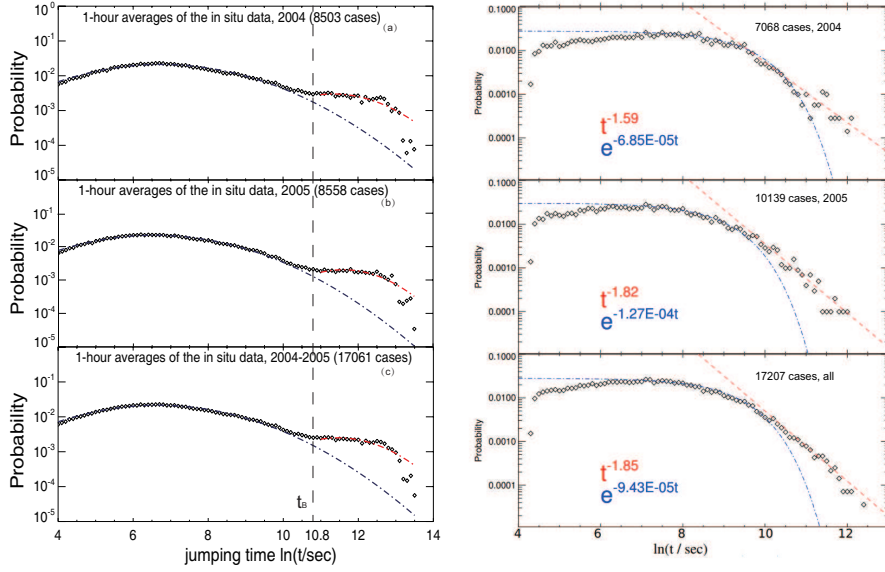


Figure 5. Left panel: Statistical analysis of jump times in different years. Panel a and b are the jump-time analysis in 2004 and 2005, respectively. Panel c is the jump-time analysis for all cases. Right panel: Statistical analysis of waiting times of current sheets with all deflection angles in different years (Miao, Peng, and Li, 2011). From top to bottom, the three panels are the waiting-time analysis in 2004, 2005, and all cases, respectively. The vertical dashed line is the time at break point, t_B . The y -axis is the logarithm of the probability density, and the x -axis is the logarithm of the jump time, $[\ln(t)]$, where t is expressed in seconds.

also found by Burlaga and Szabo (1999) and Burlaga (2001), who obtained the distributions of fluctuations of basic plasma fields at 1 AU (with hour averages of the density, temperature, and speed), which also tend to be approximate log-normal distributions for a one-year interval. We also found that the width of the log-normal distributions for 2004 and 2005 and the sum are almost the same. Comparing this with the right panel of Figure 5, we find that on a short time-scale, the distribution of the jump times between magnetic cells is similar to the distribution of the waiting times of *in-situ* current sheets; on a long time-scale, however, they appear to be different. The longer waiting times of the *in-situ* current sheets resemble power laws, while the footpoint jump times are still best fitted by a log-normal.

Next we examined the jump-time statistics of footpoints that cross the boundaries of magnetic cells. These jump times are a subset of the above study. Figure 6 shows their distribution. Compared with Figure 5, the distributions are similar. This suggests that there is no obvious difference when the jump crosses the boundary or when it does not; therefore, this result supports the scenario that the current sheets may originate from the same mechanism. The average jump time of footpoints that cross the boundaries of magnetic cells ($\approx e^{8.08}$ seconds) is longer than the average jump time of all footpoints ($\approx e^{6.65}$ seconds). We note that the average jump times crossing magnetic cells in Figure 6 (from top to bottom) on a long time-scale are $\approx e^{11.23}$ seconds, $\approx e^{11.56}$ seconds, $\approx e^{11.38}$ seconds; these are roughly the same as the average time of all footpoints in

Figure 5. Furthermore, the curves are not fitted well on a short time-scale (when $t < \approx e^{6.25}$ seconds) as in Figure 5. Indeed, the observations showed a higher probability than the fitted curve. One possible reason is that the footpoints are more clustered near cell boundaries, which leads to more small-scale jump times.

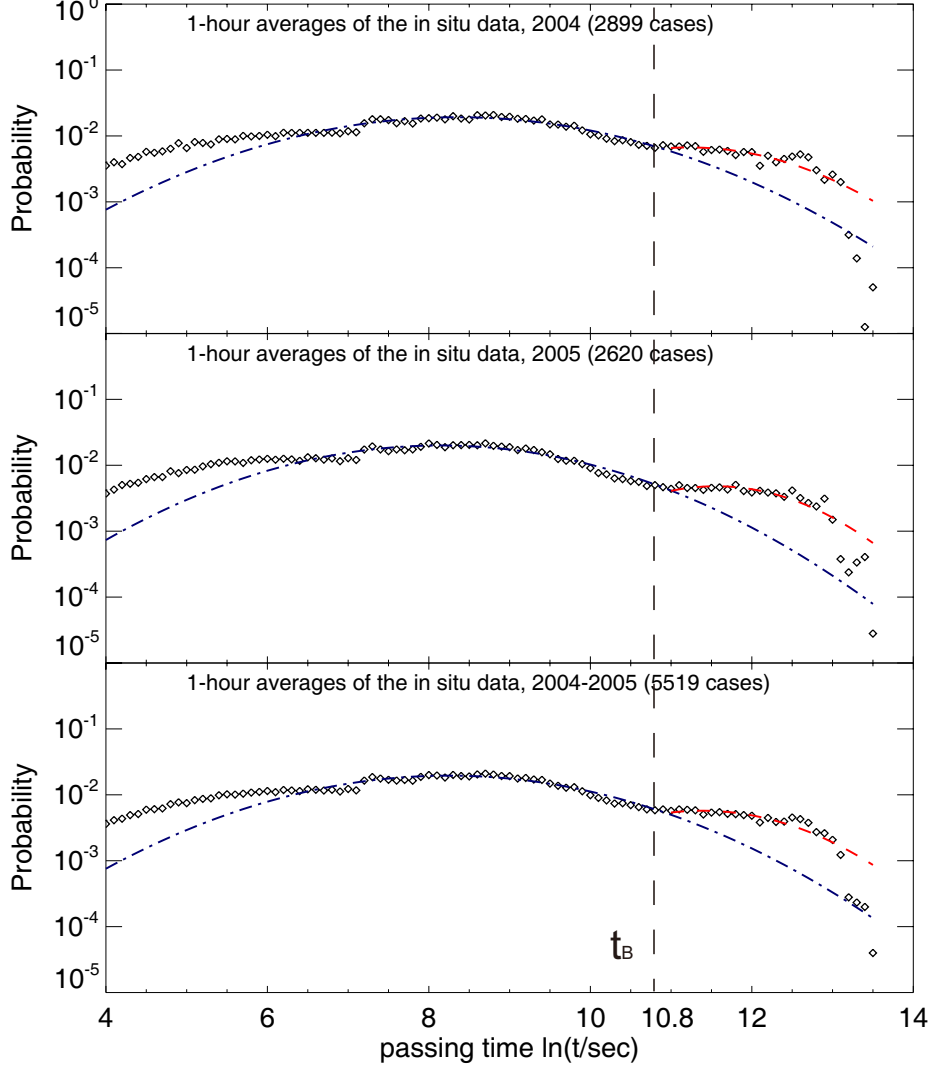


Figure 6. Statistical analysis of the jump times when jumps are crossing the boundary of the magnetic network in different years. From top to bottom, they are for 2004, 2005, and both years, respectively. The y -axis is the logarithm of the probability density and the x -axis is the logarithm of jump time, $[\ln(t)]$, where t is expressed in seconds.

Miao, Peng, and Li (2011) used a statistical analysis of the waiting time of current sheets from the *Ulysess* data, and suggested that for all angle analyses (Miao, Peng, and Li, 2011, Figure 9), the distributions behave like exponential

decays on short time-scales and power laws when $t > \lambda$ [λ is the breakpoint of the waiting time].

In our case, we found that the result agrees with the result of waiting times of current sheets Greco *et al.* (2009); Miao, Peng, and Li (2011); the PDF of the jump times of photospheric footpoints behaves like a combination of two approximate log-normal distributions, one on a short time-scale (when $t < t_B$, where t_B is the break point of the jump time) and the other on a long time-scale (when $t > t_B$). This represents that the large-angle current sheets may originate from a different mechanism from the small-angle population. The first approximate log-normal distribution is similar to the result of Miao, Peng, and Li (2011); this result shows that there are perhaps small-angle current sheets that developed in the solar-wind MHD turbulence, as shown by Zhou, Matthaeus, and Dmitruk (2004) and Chang, Tam, and Wu (2004). Therefore, these current sheets may represent the intrinsic intermittency of the solar-wind MHD turbulence. We suggest that the second log-normal distribution is that of the current sheets with a large deflection angle; this supports the conjecture that solar-wind turbulent fluctuations are at least in part related to the presence of large structures of highly conducting plasma, *i.e.* the flux tubes in the solar wind.

4. Conclusion

Previous studies by Bruno *et al.* (2004) and Miao, Peng, and Li (2011) have suggested that there are two populations of current sheets in the solar wind, one of which with large deflection angles and maybe related to flux-tube boundaries.

To examine the origin of these large-angle current sheets, we traced back the solar wind to the solar surface and together with the magnetic-cell map using the procedure presented by Huang *et al.* (2012), we examined the jump times between adjacent footpoints. We identified a total of 17 061 jumps for 2004 and 2005. Of these, 5519 have boundary crossings. The PDF of the jump times are shown in Figure 5 and Figure 6. These results showed that there are two populations of the jump times, one on a short jump time-scale and one on a long jump time-scale. Both of them can be fitted by log-normals. We also found that the average jump time of footpoints that cross the boundaries of the magnetic network is longer than the average jump time of all the footpoints; this is consistent with the findings of Miao, Peng, and Li (2011), who reported that the waiting times of current sheets with all deflection angles are shorter than current sheets with large deflection angles. These results support the view that the large-angle population of current sheets may originate from a mechanism different from that of the small-angle population, and confirm that there might be a physical connection between the flux tube at the solar surface and the large current sheet observed from the *in-situ* data.

Acknowledgements SOHO is a project of international cooperation between ESA and NASA. The solar-wind data used in this work are from the *Wind* and ACE teams. This work is supported by NSFC grant Nos. 11221063, 11211120147, 11103039, 11103044 and 11273030, MOST grant No. 2011CB811401, Marie Curie Actions IRSES-295272-RADIOSUN and the

National Major Scientific Equipment R&D Project ZDYZ2009-3. G L's work at UA Huntsville was supported by NSF grants ATM-0847719 and AGS-0962658. We also thank the referee for very helpful comments.

References

- Altschuler, M.D., Newkirk, G.: 1969, Magnetic Fields and the Structure of the Solar Corona. I: Methods of Calculating Coronal Fields. *Solar Phys.* **9**, 131. DOI.
- Bartley, W.C., Bukata, R.P., McCracken, K.G., Rao, U.R.: 1966, Anisotropic cosmic radiation fluxes of solar origin. *J. Geophys. Res.* **71**, 3297. DOI.
- Borovsky, J.E.: 2008, Flux tube texture of the solar wind: Strands of the magnetic carpet at 1 AU? *J. Geophys. Res.* **113**, A08110. DOI.
- Bruno, R., Carbone, V.: 2005, The Solar Wind as a Turbulence Laboratory. *Liv Rev. Solar Phys.* **2**, 4. DOI.
- Bruno, R., Burlaga, L.F., Hundhausen, A.J.: 1982, Quadrupole distortions of the heliospheric current sheet in 1976 and 1977. *J. Geophys. Res.* **87**, 10339. DOI.
- Bruno, R., Burlaga, L.F., Hundhausen, A.J.: 1984, K-coronameter observations and potential field model comparison in 1976 and 1977. *J. Geophys. Res.* **89**, 5381. DOI.
- Bruno, R., Carbone, V., Veltri, P., Pietropaolo, E., Bavassano, B.: 2001, K-coronameter observations and potential field model comparison in 1976 and 1977. *Planetary Space Sci.* **49**, 1201. DOI.
- Bruno, R., Carbone, V., Primavera, L., Malara, F., Sorriso-Valv, L., Bavassano, B.: 2004, On the probability distribution function of small-scale interplanetary magnetic field fluctuations. *Ann. Geophys.* **22**, 3751. DOI.
- Burlaga, L.F.: 2001, Lognormal and multifractal distributions of the heliospheric magnetic field. *J. Geophys. Res.* **106**, 15917. DOI.
- Burlaga, L.F., Szabo, A.: 1999, Fast and Slow Flows in the Solar Wind Near the Ecliptic at 1 AU? *Space Sci. Rev.* **87**, 137. DOI.
- Chang, T., Tam, S., Wu, C.: 2004, Complexity induced anisotropic bimodal intermittent turbulence in space plasmas. *Phys. Plasmas* **11**, 1287. DOI.
- Goldstein, M.L., Roberts, D.A., Matthaeus, W.H.: 1995, Magnetohydrodynamic Turbulence In The Solar Wind. *Astron. Astrophys. Rev.* **33**, 283. DOI.
- Greco, A., Matthaeus, W.H., Servidio, S., Dmitruk, P.: 2009, Waiting-time distributions of magnetic discontinuities: Clustering or Poisson process? *Phys. Rev. E* **80**, 046401. DOI.
- Hapgood, M.A.: 1992, Space physics coordinate transformations - A user guide. *Planetary Space Sci.* **40**, 711. DOI.
- Hirzberger, J., Gizon, L., Solanki, S.K., Duvall, T.L.: 2008, Structure and Evolution of Supergranulation from Local Helioseismology. *Solar Phys.* **251**, 417. DOI.
- Huang, C., Yan, Y.H., Zhang, Y., Tan, B.L., Li, G.: 2012, The Morphologic Properties of Magnetic Networks over the Solar Cycle 23. *Astrophys. J.* **759**, 106. DOI.
- Kolmogorov, A.: 1941, The Local Structure of Turbulence in Incompressible Viscous Fluid for Very Large Reynolds' Numbers. *C. R. Acad. Sci. URSS* **30**, 301. DOI.
- Lemen, J.R., Title, A.M., Akin, D.J., Boerner, P.F., Chou, C., Drake, e. J. F.: 2012, The Atmospheric Imaging Assembly (AIA) on the Solar Dynamics Observatory (SDO). *Solar Phys.* **275**, 17. DOI.
- Lepping, R.P., Acuña, M.H., Burlaga, L.F., Farrell, W.M., Slavin, J.A., Schatten, e. K. H.: 1995, The Wind Magnetic Field Investigation. *Space Sci. Rev.* **71**, 207. DOI.
- Li, G.: 2007, Flux tubes in the fast and slow solar wind. In: Shaikh, D., Zank, G.P. (eds.) *Turbulence and Nonlinear Processes in Astrophysical Plasmas* **CS-932**, Amer. Inst. Phys, ???, 206. DOI.
- Li, G.: 2008, Identifying Current-Sheet-like Structures in the Solar Wind. *Astrophys. J. Lett.* **672**, L65. DOI.
- Li, G., Lee, E., Parks, G.: 2008, Are there current-sheet-like structures in the Earth's magnetotail as in the solar wind - results and implications from high time resolution magnetic field measurements by Cluster. *Ann. Geophys.* **26**, 1889. DOI.
- Mariani, F., Bavassano, B., Villante, U., Ness, N.: 1973, Variations of the occurrence rate of discontinuities in the interplanetary magnetic field. *J. Geophys. Res.* **78**, 8011. DOI.

- McComas, D.J., Bame, S.J., Barker, P.L., Delapp, D.M., Feldman, W.C., Gosling, e. J. T.: 1998, An unusual coronal mass ejection: First solar wind electron, proton, alpha monitor (SWEPAM) Results from the Advanced Composition Explore. *Geophys. Res. Lett.* **25**, 4289. DOI.
- McCracken, K., Ness, N.: 1966, The Collimation of Cosmic Rays by the Interplanetary Magnetic Field. *J. Geophys. Res.* **71**, 3315. DOI.
- McIntosh, S.W., Leamon, R.J., de Pontieu, B.: 2011, The Spectroscopic Footprint of the Fast Solar Wind. *Astrophys. J.* **727**, 7. DOI.
- McIntosh, S.W., Innes, D.E., de Pontieu, B., Leamon, R.J.: 2010, STEREO observations of quasi-periodically driven high velocity outflows in polar plumes. *Astron. Astrophys.* **510**, L2. DOI.
- Miao, B., Peng, B., Li, G.: 2011, Current sheets from Ulysses observation. *Ann. Geophys.* **29**, 237. DOI.
- Neugebauer, M., Forsyth, R.J., Galvin, A.B., Harvey, K.L., Hoeksema, A.J., Lazarus, e. A. J.: 1998, Spatial structure of the solar wind and comparisons with solar data and models. *J. Geophys. Res.* **103**, 14587. DOI.
- Ogilvie, K.W., Chornay, D.J., Fritzenreiter, R.J., Hunsaker, F., Keller, J., Lobell, e. J.: 1995, SWE, A Comprehensive Plasma Instrument for the Wind Spacecraft. *Ann. Geophys.* **71**, 55. DOI.
- Schatten, K.H., Wilcox, J.M., Ness, N.F.: 1969, A model of interplanetary and coronal magnetic fields. *Solar Phys.* **6**, 442. DOI.
- Scherrer, P.H., Bogart, R.S., Bush, R.I., Hoeksema, J.T., Kosovichev, A.G., Schou, e. J.: 1995, The Solar Oscillations Investigation - Michelson Doppler Imager. *Solar Phys.* **162**, 129. DOI.
- Schrijver, C.J.: 2001, Simulations of the Photospheric Magnetic Activity and Outer Atmospheric Radiative Losses of Cool Stars Based on Characteristics of the Solar Magnetic Field. *Astrophys. J.* **547**, 475. DOI.
- Schrijver, C.J., De Rosa, M.L.: 2003, Photospheric and heliospheric magnetic fields. *Solar Phys.* **212**, 165. DOI.
- Sun, X., Hoeksema, J.T., Liu, Y., Wiegmann, T., Hayashi, K., Chen, e. Q.: 2012, Evolution of Magnetic Field and Energy in a Major Eruptive Active Region Based on SDO/HMI Observation. *Astrophys. J.* **748**, 77. DOI.
- Trenchi, L., Bruno, R., D'Amicis, R., Marcucci, M.F., Telloni, D.: 2013a, Observations of IMF coherent structures and their relationship to SEP dropout events. *Ann. Geophys.* **31**, 1333. DOI.
- Trenchi, L., Bruno, R., Telloni, D., D'Amicis, R., Marcucci, M.F., Zurbuchen, e. T. H.: 2013b, Solar Energetic Particle Modulations Associated with Coherent Magnetic Structures. *Astrophys. J.* **770**, 11. DOI.
- Tu, C.-Y., Marsch, E.: 1995, MHD structures, waves and turbulence in the solar wind: Observations and theories. *Space Sci. Rev.* **73**, 1. DOI.
- Veltri, P., Mangeney, A.: 1999, Scaling laws and intermittent structures in solar wind MHD turbulence. In: Habbal, S. (ed.) *Solar Wind Nine: Proceedings of the Ninth International Solar Wind Conference CS-471*, Amer. Inst. Phys., ???, 543. DOI.
- Wang, H.M., Zirin, H.: 1989, Study of supergranules. *Solar Phys.* **120**, 1. DOI.
- Zhou, Y., Matthaeus, W., Dmitruk, P.: 2004, Colloquium: Magnetohydrodynamic turbulence and time scales in astrophysical and space plasmas. *Rev. Mod. Phys.* **76**, 1015. DOI.